



ISTITUTO NAZIONALE DI RICERCA METROLOGICA Repository Istituzionale

Enhancing domain wall velocity through interface intermixing in W-CoFeB-MgO films with perpendicular anisotropy

Original

Enhancing domain wall velocity through interface intermixing in W-CoFeB-MgO films with perpendicular anisotropy / Zhao, Xiaoxuan; Zhang, Boyu; Vernier, Nicolas; Zhang, Xueying; Sall, Mamour; Xing, Tao; Diez, Liza Herrera; Hepburn, Carolyn; Wang, Lin; Durin, Gianfranco; Casiraghi, Arianna; Belmeguenai, Mohamed; Roussigné, Yves; Stashkevich, Andrei; Chérif, Salim Mourad; Langer, Jürgen; Ocker, Berthold; Jaiswal, Samridh; Jakob, Gerhard; Kläui, Mathias; Zhao, Weisheng; Ravelosona, Dafiné. - In: APPLIED PHYSICS LETTERS. - ISSN 0003-6951. - 115:12(2019), p. 122404. [10.1063/1.5121357]

This version is available at: 11696/61425 since: 2020-02-21T17:12:46Z

Publisher:

Published

DOI:10.1063/1.5121357

Terms of use:

This article is made available under terms and conditions as specified in the corresponding bibliographic description in the repository

Publisher copyright

(Article begins on next page)

Enhancing domain wall velocity through interface intermixing in W-CoFeB-MgO films with perpendicular anisotropy

Cite as: Appl. Phys. Lett. **115**, 122404 (2019); <https://doi.org/10.1063/1.5121357>

Submitted: 24 July 2019 . Accepted: 02 September 2019 . Published Online: 20 September 2019

Xiaoxuan Zhao, Boyu Zhang, Nicolas Vernier, Xueying Zhang, Mamour Sall, Tao Xing, Liza Herrera Diez, Carolyn Hepburn, Lin Wang, Gianfranco Durin, Arianna Casiraghi , Mohamed Belmeguenai , Yves Roussigné , Andrei Stashkevich, Salim Mourad Chérif, Jürgen Langer , Berthold Ocker , Samridh Jaiswal , Gerhard Jakob , Mathias Kläui, Weisheng Zhao , and Dafiné Ravelosona 



View Online



Export Citation



CrossMark

ARTICLES YOU MAY BE INTERESTED IN

[Spin-orbit torques and their angular dependence in ferromagnet/normal metal heterostructures](#)

Applied Physics Letters **115**, 122405 (2019); <https://doi.org/10.1063/1.5117353>

[High spin-wave propagation length consistent with low damping in a metallic ferromagnet](#)

Applied Physics Letters **115**, 122402 (2019); <https://doi.org/10.1063/1.5102132>

[Efficient spin current generation in low-damping Mg\(Al, Fe\)₂O₄ thin films](#)

Applied Physics Letters **115**, 122401 (2019); <https://doi.org/10.1063/1.5119726>



Lock-in Amplifiers

Zurich Instruments

Watch the Video

Enhancing domain wall velocity through interface intermixing in W-CoFeB-MgO films with perpendicular anisotropy

Cite as: Appl. Phys. Lett. **115**, 122404 (2019); doi: [10.1063/1.5121357](https://doi.org/10.1063/1.5121357)

Submitted: 24 July 2019 · Accepted: 2 September 2019 ·

Published Online: 20 September 2019



View Online



Export Citation



CrossMark

Xiaoxuan Zhao,^{1,2} Boyu Zhang,¹ Nicolas Vernier,² Xueying Zhang,^{1,3,4} Mamour Sall,² Tao Xing,^{1,3} Liza Herrera Diez,² Carolyna Hepburn,² Lin Wang,^{3,4} Gianfranco Durin,⁵ Arianna Casiraghi,⁵ Mohamed Belmeguenai,⁶ Yves Roussigné,⁶ Andrei Stashkevich,⁶ Salim Mourad Chérif,⁶ Jürgen Langer,⁷ Berthold Ocker,⁷ Samridh Jaiswal,^{7,8} Gerhard Jakob,⁸ Mathias Kläui,⁸ Weisheng Zhao,^{1,3,a)} and Dafiné Ravelosona^{2,9,a)}

AFFILIATIONS

¹Fert Beijing Institute, School of Microelectronics, Beihang University, 100191 Beijing, China

²Centre de Nanosciences et de Nanotechnologies, CNRS, University Paris-Sud, Université Paris-Saclay, 10 Boulevard Thomas Gobert, 91405 Orsay, France

³Beihang-Goertek Joint Microelectronics Institute, Qingdao Research Institute, Beihang University, 266000 Qingdao, China

⁴Truth Instrument Co. Ltd., 266000 Qingdao, China

⁵Instituto Nazionale di Ricerca Metrologica, Strada delle Cacce 91, 10135 Torino, Italy

⁶LSPM (CNRS-UPR 3407), Université Paris 13, Sorbonne Paris Cité, 99 Avenue Jean-Baptiste Clément, 93430 Villetaneuse, France

⁷Singulus Technology AG, Hanauer Landstrasse 103, 63796 Kahl am Main, Germany

⁸Institute of Physics, Johannes Gutenberg University Mainz, 55099 Mainz, Germany

⁹Spin-Ion Technologies, 10 Boulevard Thomas Gaubert, 91120 Palaiseau, France

^{a)} Authors to whom correspondence should be addressed: weisheng.zhao@buaa.edu.cn and dafine.ravelosona@c2n.upsaclay.fr

ABSTRACT

We study the influence of He⁺ irradiation induced interface intermixing on magnetic domain wall (DW) dynamics in W-CoFeB (0.6 nm)-MgO ultrathin films, which exhibit high perpendicular magnetic anisotropy and large Dzyaloshinskii-Moriya interaction (DMI) values. Whereas the pristine films exhibit strong DW pinning, we observe a large increase in the DW velocity in the creep regime upon He⁺ irradiation, which is attributed to the reduction of pinning centers induced by interface intermixing. Asymmetric in-plane field-driven domain expansion experiments show that the DMI value is slightly reduced upon irradiation, and a direct relationship between DMI and interface anisotropy is demonstrated. Our findings provide insights into the material design and interface control for DW dynamics, as well as for DMI, enabling the development of high-performance spintronic devices based on ultrathin magnetic layers.

Published under license by AIP Publishing. <https://doi.org/10.1063/1.5121357>

Domain wall (DW) dynamics in ultrathin films with perpendicular magnetic anisotropy (PMA) is of great interest for the realization of low-power high-performance memory and logic devices.^{1,2} The combination of the spin-orbit torque (SOT) resulting from the spin Hall effect (SHE) and the Dzyaloshinskii-Moriya interaction (DMI) at interfaces between heavy metals (HMs) and ferromagnetic layers has been demonstrated to be a powerful means to drive efficiently domain-wall^{3,4} and skyrmion^{5,6} motion, which are expected to be the promising new generation of information carriers owing to ultralow driving currents. However, the crucial limitation of SOT induced

chiral DW or skyrmion motion results from the presence of pinning defects, which induces large threshold currents and stochastic behaviors. Such an important role of magnetic inhomogeneities in the current-induced motion of skyrmions has been revealed in recent studies,⁷⁻⁹ taking into account a distribution of magnetic properties in a granular magnetic media where the grain size is comparable to the skyrmion diameter. One important source of disorder is related to the atomic-scale properties of the interface where roughness or interface intermixing^{10,11} can not only induce a spatial distribution of interface anisotropy but also interfacial DMI. Recently, Zimmermann *et al.*¹⁰

employed *ab initio* calculations to study the effect of intermixing on DMI at Co/Pt interfaces, finding that the DMI dropped by about 20% and remained constant for a broad range of degrees of intermixing. In another study,¹² *ab initio* calculations show that a 25% interfacial mixing at the Co/Pt interface reduced the total DMI value by half. These calculations take only the nearest neighbors into account, leading to a gap between simulation results and experimental conditions. In addition, previous studies^{13,14} have shown that asymmetric disorder between the bottom and top interfaces in the heavy metal (HM)/ferromagnetic metal (FM)/oxide or HM structure can lead to an increase in the DMI. These studies clearly show that understanding and minimizing the role of interface disorder are crucial for the design of future low power devices based on chiral DW motion and skyrmion manipulation.

In this work, we study the influence of interface intermixing on DW dynamics in W-CoFeB (0.6 nm)-MgO films that exhibit high PMA and a large DMI value. Such a system shows great potential not only for SOT based memory devices¹⁵ but also for spin Hall nano-oscillators and spin Hall generation of propagating spin waves owing to its high PMA and large spin Hall angle.^{16,17} We show that opposite to the Ta-CoFeB-MgO system,^{14,18} a weak intermixing of the bottom W-CoFeB interface leads to a strong reduction of DW pinning and an increase in DW velocity in the creep regime, whereas the DMI value is only slightly reduced. The reduction of DMI is also found to be correlated with the reduction of interface anisotropy.

The investigated samples are W(4 nm)/Co₂₀Fe₆₀B₂₀(0.6 nm)/MgO(2 nm)/Ta(3 nm) structures [Fig. 1(a)], grown on top of oxidized silicon substrates using a “Singulus Rotaris” deposition system. The samples were annealed at 400 °C for 2 h. Then, the samples were irradiated by He⁺ ions with an energy of 15 keV and fluences (irradiation doses, ID) ranging from 2×10^{18} to 3×10^{19} ions/m². As demonstrated in previous studies, the use of light He⁺ irradiation at energies in the range of 10–30 keV induces short range atomic displacements (absence of cascade collisions) without generating defects in the materials (absence of cascade collisions) as in the case of irradiation with heavier Ar⁺ or Ga⁺ ions.

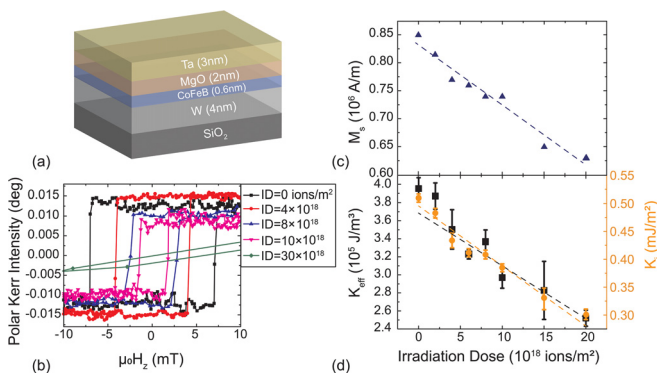


FIG. 1. (a) Schematic diagram of the investigated structure. (b) Hysteresis loops of irradiated samples for different irradiation fluences (IDs). (c) Saturation magnetization M_s as a function of fluence. (d) Effective anisotropy (black triangles) and interface anisotropy (orange dots) as a function of fluence. Error bars correspond to uncertainties in the estimation of the anisotropy field H_k .

As shown in Fig. 1(b), the coercive field is reduced when increasing the He⁺ fluence, and for the largest dose of 3×10^{19} He⁺/m², the easy axis of magnetization lies in-plane. Figures 1(c) and 1(d) show the saturation magnetization M_s , the effective anisotropy $K_{eff} = \frac{1}{2} \mu_0 M_s H_k$, where H_k is the anisotropy field, and the interface anisotropy $K_i = (K_{eff} + \mu_0 M_s^2 / 2) \times t_{FM}$. M_s and H_k were measured by superconducting quantum interference device (SQUID) magnetometry under perpendicular and in-plane magnetic fields, respectively. Upon irradiation, M_s , K_{eff} , and K_i show a linear reduction as a function of fluence. This is consistent with our previous study on Ta-CoFeB (1 nm)-MgO systems where the main effect of ion irradiation is to induce Fe diffusion into Ta (intermixing at the bottom interface), while the top CoFeB-MgO interface is more robust upon intermixing (Fe-Mg and Co-Mg have a positive enthalpy of mixing).¹⁸ Here also, the reduction of M_s is consistent with a diffusion of Fe into the W layer due to a negative enthalpy of mixing.¹⁹ As for Ta-Fe alloys, which formed a dead layer at the CoFeB-Ta interface,^{20–22} W-Fe alloys are also expected to be paramagnetic for a low concentration of Fe.²³ This explains that the overall magnetization is linearly reduced upon irradiation induced intermixing at the W-CoFeB interface. In addition, the primary source of reduction of interfacial anisotropy upon irradiation is related to the diffusion of Fe from the top CoFeB-MgO interface to the W layer, reducing the hybridization between the Fe-3d and O-2p orbitals.²⁴ This also explains the reduction of coercive fields seen in Fig. 1(b). Indeed, as shown by Kerr microscopy measurements, the magnetization reversal is dominated by nucleation of reversed domains at some specific locations followed by rapid DW propagation. Thus, the coercive field here corresponds to the nucleation field. As nucleation field depends on the anisotropy,²⁵ the reduction of the coercivity fields upon irradiation is linked to the reduction of anisotropy. It is also worth noting that a higher fluence is needed for the magnetization to go in-plane for W-CoFeB (0.6 nm)-MgO (ID = 3×10^{19} ions/m²) than for Ta-CoFeB (1 nm)-MgO (ID = 1.5×10^{19} ions/m²) in spite of the thinner magnetic layer. This is consistent with the fact that the enthalpy of mixing of W-Fe is less negative than that of Ta-Fe, i.e., W is more robust to intermixing than Ta.

To address the effect of He⁺ irradiation induced interface intermixing on DW dynamics, the DW velocity has been measured by Kerr microscopy for different fluences up to 1×10^{19} ions/m². Note that above this fluence, the interface anisotropy energy is too low, leading to a spontaneous demagnetized state, where it is impossible to get a stable domain bubble. The domain wall velocity has been determined by measuring the average displacement of bubble-like domains under perpendicular magnetic field pulses H_z with the pulse duration ranging from 3 μ s to 10 s. All measurements were conducted at room temperature. The typical image of a magnetic domain after expansion under a perpendicular field is presented in Fig. 2(a). The DW velocity plotted on a logarithmic scale in Fig. 2(b) is given by the universal creep law²⁶

$$v = v(H_{dep}) \exp \left[-\frac{U_C}{k_B T} \left(\left(\frac{H_{dep}}{H_z} \right)^\mu - 1 \right) \right], \quad (1)$$

where U_C is the scaling energy constant, k_B is the Boltzmann constant, T is the temperature, H_{dep} is the depinning field at 0 K, and $\mu = 1/4$ is the critical exponent. This thermally activated regime describes the collective pinning of the DW by structural defects present in the ultra-thin films. For high fields, too many nucleation events occur, which

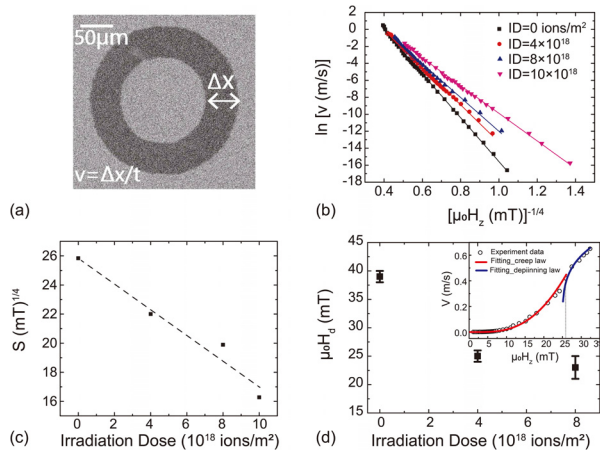


FIG. 2. (a) Typical image of DW expansion under a field pulse allowing the measurement of DW velocity. (b) DW velocity as a function of perpendicular magnetic field $H_z^{-1/4}$ for different fluences. (c) Coefficient S [linear slope of the DW velocity vs field seen in (b)] as a function of the irradiation fluences. (d) Value of H_{dep} as a function of fluence. The inset shows the fitting procedure to determine H_{dep} as described in the text.

makes it difficult to measure the DW velocity. As seen in Fig. 2(b), the main result of this study is a strong increase in the DW velocity in the creep regime upon He^+ irradiation induced intermixing.

This result is opposite to that of Ta-CoFeB-MgO systems, where irradiation induced intermixing leads to a strong reduction of DW velocity due to an increase in the pinning potential. To provide a deeper understanding of the increase in DW velocity in the creep regime, as illustrated in Fig. 2(c), we have plotted

$$S = \left(\frac{U_C}{k_B T} \right) H_{dep}^{\mu} \quad (2)$$

as a function of fluence, which represents the slope of the linear variation seen in Fig. 2(b). The slope S shows a linear reduction as a function of the fluence, which is consistent with a progressive increase in DW velocity at a given field. H_{dep} is usually estimated by determining the intersection between the creep and the intermediate depinning regime using a fitting procedure.^{26,27} We apply this procedure here but taking into account that the intermediate depinning regime above the creep regime is very limited since it was not possible to measure DW velocity at very high fields due to nucleation events [see the inset of

Fig. 2(d)]. As seen in Fig. 2(d), a strong reduction of H_{dep} from 40 to 20 mT is observed upon irradiation, indicating a decrease in the pinning potential strength. As described in Ref. 18, H_{dep} includes a dependence on magnetic anisotropy K_{eff} , saturation magnetization M_s , and the pinning density n_i through

$$H_{dep} \propto \frac{\sqrt{K_{eff}} n_i^{2/3}}{M_s} \quad (3)$$

From the value of M_s and K_{eff} , which both decrease upon irradiation, we can deduce that the reduction of H_{dep} by a factor of 2 is mainly driven by the reduction of the pinning density n_i since the ratio K_{eff}^2/M_s is nearly constant from $ID = 0$ to $ID = 10 \times 10^{18}$ ions/m². In addition, by considering the value of H_{dep} in Eq. (2), the reduction of the parameter S is also found to be mainly driven by the reduction of H_{dep} since $\frac{U_C}{k_B T}$ is nearly constant (varying from 15 to 12).

The increase in domain wall velocity is then correlated with a reduction of the density of the pinning centers in our samples driven by ion irradiation induced intermixing. This is opposite to the Ta-CoFeB (1 nm)-MgO case where irradiation induced intermixing leads to a strong increase in DW pinning. In order to explain this result, we first note that the DW velocity in the nonirradiated Ta-CoFeB (1 nm)-MgO system¹⁸ is 1–2 orders of magnitude larger than that of W-CoFeB (0.6 nm)-MgO at a given field for similar K_{eff} and M_s values. This is related to a higher pinning strength in pristine W-CoFeB (0.6 nm)-MgO structures as illustrated by the different H_{dep} values [$H_{dep} = 8$ mT (Ref. 18) and $H_{dep} = 40$ mT for Ta-CoFeB-MgO and W-CoFeB-MgO systems, respectively]. Beyond the fact that a 0.6 nm thick magnetic layer is more disordered than a 1 nm thick layer, our further assumption is that since the W-CoFeB interface is less sensitive to intermixing than the Ta-CoFeB interface, the interface disorder may be dominated by roughness in pristine W-CoFeB-MgO structures (flat terraces separated by atomic steps at the W-CoFeB interface) and by intermixing in thicker Ta-CoFeB-MgO structures. Since the strength of pinning is higher for atomic steps,²⁸ this can explain the difference in domain wall velocity with respect to the pristine films. As sketched in Fig. 3, upon irradiation, intermixing is induced at the W-CoFeB interface, erasing the atomic steps and smoothening the interface. This leads to a reduction of the pinning consistent with the increase in DW velocity.

To further investigate the effects of interface disorder on magnetic properties, we have also studied the influence of intermixing on the Dzyaloshinskii-Moriya interaction. We have used magnetic bubble

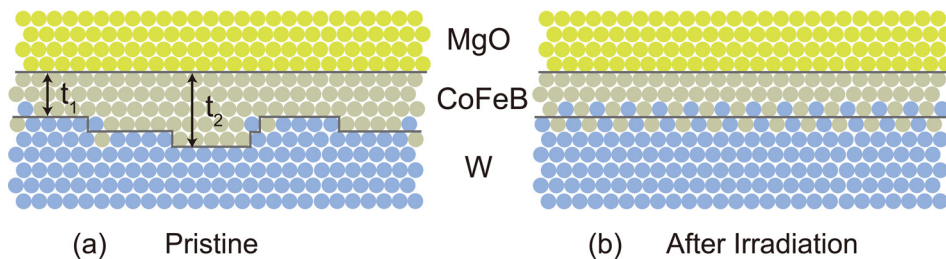


FIG. 3. Schematic of the interface structure in (a) pristine and (b) irradiated W-CoFeB-MgO films. The dots in yellow represent the MgO layer, while those in gray and blue correspond to the CoFeB and W layers, respectively. Before irradiation, the interface disorder is dominated by roughness (terraces separated by atomic steps), whereas after irradiation, interface disorder is related to intermixing.

expansion in the creep regime under both perpendicular and in-plane magnetic fields. As shown in Fig. 4(a), the radial symmetry is broken due to the presence of an internal effective DMI field.²⁹ By measuring the DW velocity in both directions along the x axis, the effective H_{DMI} field can be estimated. The DMI constant D is then directly calculated from $\mu_0 H_{DMI} = D/M_s \Delta$, where Δ is the DW width defined by $\sqrt{A/K_{eff}}$, with A being the exchange stiffness constant, taken here as 15 pJ/m (Ref. 30) and assumed to be constant for all samples. For the pristine sample, we find a DMI field of 58 ± 4 mT, which corresponds to a DMI constant of 0.30 ± 0.022 mJ/m², and a right-handed magnetic chirality, in agreement with previous studies on W-CoFeB-MgO films.³¹ Figure 4(b) shows the DMI value as a function of the fluence up to 1×10^{19} ions/m², where a slight linear decrease is observed from 0.30 ± 0.02 to 0.21 ± 0.02 upon intermixing. It has been shown that the CoFeB/W interface exhibits a positive DMI constant,³² while the MgO/CoFeB interface has the opposite sign.^{32,33} As we have shown, the main effect of ion irradiation is to induce intermixing at the bottom heavy metal (HM)/ferromagnetic metal (FM) interface. Such intermixing modifies the atomic environment of magnetic and heavy metal atoms at the interface (from interface roughness to intermixing), which reduces the DMI value as shown in previous studies.^{10,12} In particular, interface DMI is expected to be higher for a rough interface [Fig. 3(a)] than for an intermixed interface [Fig. 3(b)] since pairwise interaction between 2 magnetic atoms mediated by a heavy metal atom is maximized. Our results are in line with those of Tacchi *et al.*,³⁴ which demonstrate a DMI enhancement with the Pt thickness in Pt/CoFeB systems due to cumulative itinerant electron hopping between

the atomic spins at the interface and the nonmagnetic atoms in the heavy metal. In our case, the allowing of the W layer with Fe at the bottom interface reduces the scattering of itinerant electrons with the HM, resulting in an overall reduction of DMI. As a result, the bottom interfacial DMI is weakened, leading to a reduction of the overall still positive DMI.

Finally, the interfacial anisotropy K_i and the DMI value having the same units (millijoule per square meter) are plotted as a function of the fluence on the same graph as seen in Fig. 4(b). First, we can notice that both K_i and DMI exhibit a linear decrease vs ID with a very similar trend. Considering the slope coefficient β_{K_i} and β_{DMI} , defined as the relative change in K_i and DMI constant over the change in the irradiation fluence, namely, $\Delta K_i / \Delta ID$ and $\Delta DMI / \Delta ID$, respectively, we find $\beta_{K_i} = 0.0121$ mJ/10¹⁸ ions and $\beta_{DMI} = 0.0094$ mJ/10¹⁸ ions. This direct relationship between the relative variation of DMI and interface anisotropy upon intermixing indicates that they have the same origin, the exchange interaction between magnetic and heavy metal atoms mediated by spin-orbit coupling.^{35–37}

In summary, we have studied the influence of He⁺ irradiation-induced interfacial intermixing on domain wall dynamics and Dzyaloshinskii-Moriya interaction. We have observed a large increase in domain wall velocity in the creep regime which is consistent with a reduction of pinning at the W/CoFeB interface. A slight reduction of the DMI value is found upon irradiation, and a direct relationship with the interface anisotropy K_i is demonstrated. Only an irradiation dose of 4×10^{18} ions/m² is needed to reduce the depinning field by a factor of 2, keeping a high value for the anisotropy and the DMI. Our results open a path to finely tune DMI and domain wall dynamics in ultrathin magnetic films using atomic scale control of intermixing through light He⁺ irradiation. These results are also interesting for spin Hall nano-oscillators and spin Hall generation of propagating spin waves for which a precise control of PMA and DMI is crucial.

We gratefully acknowledge the French ANR Elecspin, the Prematuration CNRS project Spin-Ion, the FP7 European WALL project (ITN WALL No. 608031), the German Research Foundation (Project No. 290319996/TRR173), the National Natural Science Foundation of China (Grant No. 61627813), International Collaboration Project B16001, and the China Scholarship Council (CSC) for their financial support of this work.

REFERENCES

- S. P. Parkin, M. Hayashi, and L. Thomas, *Science* **320**, 190 (2008).
- S. H. Yang, K. S. Ryu, and S. Parkin, *Nat. Nanotechnol.* **10**, 221 (2015).
- K. S. Ryu, L. Thomas, S. H. Yang, and S. S. Parkin, *Nat. Nanotechnol.* **8**, 527 (2013).
- S. Emori, U. Bauer, S.-M. Ahn, E. Martinez, and G. S. D. Beach, *Nat. Mater.* **12**, 611 (2013).
- A. Fert, V. Cros, and J. Sampaio, *Nat. Nanotechnol.* **8**, 152 (2013).
- J. Sampaio, V. Cros, S. Rohart, A. Thiaville, and A. Fert, *Nat. Nanotechnol.* **8**, 839 (2013).
- S. Woo, K. Litzius, B. Krüger, M.-Y. Im, L. Caretta, K. Richter, M. Mann, A. Krone, R. M. Reeve, M. Weigand, P. Agrawal, I. Lemesh, M.-A. Mawass, P. Fischer, M. Kläui, and G. S. D. Beach, *Nat. Mater.* **15**, 501 (2016).
- W. Legrand, D. Maccariello, N. Reyren, K. Garcia, C. Moutafis, C. Moreau-Luchaire, S. Collin, K. Bouzehouane, V. Cros, and A. Fert, *Nano Lett.* **17**, 2703 (2017).
- V. Kim and M. W. Yoo, *Appl. Phys. Lett.* **110**, 132404 (2017).

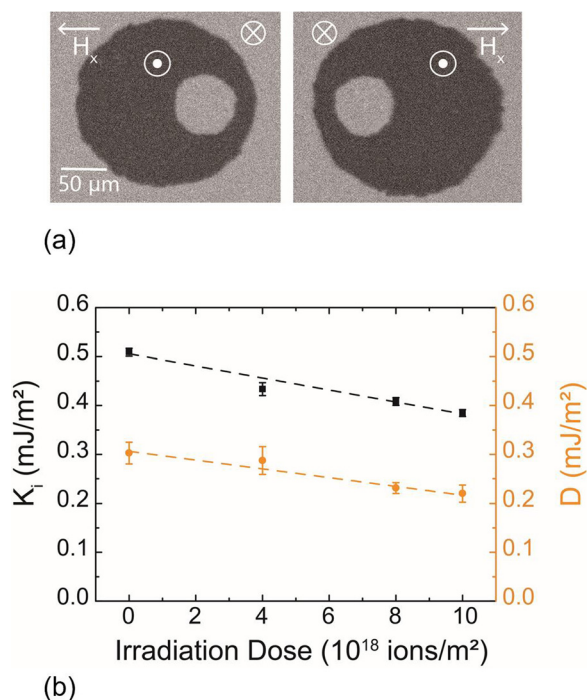


FIG. 4. (a) Differential Kerr microscopy images of the sample irradiated at 10×10^{18} ions/m² under an in-plane field of $\mu_0 H_x = \pm 23.2$ mT. (b) Interface anisotropy energy K_i (black squares) and DMI constant (orange squares) as a function of the fluence.

- ¹⁰B. Zimmermann, W. Legrand, N. Reyren, V. Cros, S. Blügel, and A. Fert, *Appl. Phys. Lett.* **113**, 232403 (2018).
- ¹¹M. Cecot, Ł. Karwacki, W. Skowroński, J. Kanak, J. Wrona, A. Zywczak, L. Yao, S. Dijken, J. Barnaś, and T. Stobiecki, *Sci. Rep.* **7**, 968 (2017).
- ¹²H. Yang, A. Thiaville, S. Rohart, A. Fert, and M. Chshiev, *Phys. Rev. Lett.* **115**, 267210 (2015).
- ¹³A. W. J. Wells, P. M. Shepley, C. H. Marrows, and T. A. Moore, *Phys. Rev. B* **95**, 054428 (2017).
- ¹⁴L. Herrera Diez, M. Voto, A. Casiraghi, M. Belmeguenai, Y. Roussigné, G. Durin, A. Lamperti, R. Mantovan, V. Sluka, V. Jeudy, Y. T. Liu, A. Stashkevich, S. M. Chérif, J. Langer, B. Ocker, L. Lopez-Diaz, and D. Ravelosona, *Phys. Rev. B* **99**, 054431 (2019).
- ¹⁵M. Wang, W. Cai, K. Cao, J. Zhou, J. Wrona, S. Peng, H. Yang, J. Wei, W. Kang, Y. Zhang, J. Langer, B. Ocker, A. Fert, and W. Zhao, *Nat. Commun.* **9**, 671 (2018).
- ¹⁶M. Zahedinejad, H. Mazraati, H. Fulara, J. Yue, S. Jiang, A. A. Awad, and J. Åkerman, *Appl. Phys. Lett.* **112**, 132404 (2018).
- ¹⁷H. Fulara, M. Zahedinejad, R. Khymyn, A. Awad, S. Muralidhar, M. Dvornik, and J. Åkerman, preprint [arXiv:1904.06945](https://arxiv.org/abs/1904.06945) (2019).
- ¹⁸L. Herrera Diez, F. García-Sánchez, J. P. Adam, T. Devolder, S. Eimer, M. S. El Hadri, A. Lamperti, R. Mantovan, B. Ocker, and D. Ravelosona, *Appl. Phys. Lett.* **107**, 032401 (2015).
- ¹⁹A. Dębski, R. Dębski, and W. Gašior, *Arch. Metall. Mater.* **59**, 1337 (2014).
- ²⁰J. Sinha, M. Gruber, M. Kodzuka, T. Ohkubo, S. Mitani, K. Hono, and M. Hayashi, *J. Appl. Phys.* **117**, 043913 (2015).
- ²¹J. Sinha, M. Hayashi, A. J. Kellock, S. Fukami, M. Yamanouchi, H. Sato, S. Ikeda, S. Mitani, S. H. Yang, S. S. P. Parkin, and H. Ohno, *Appl. Phys. Lett.* **102**, 242405 (2013).
- ²²S. Ingvarsson, G. Xiao, S. S. Parkin, and W. Gallagher, *J. Magn. Magn. Mater.* **251**, 202 (2002).
- ²³A. Nicolenco, N. Tsyntaru, J. Fornell, E. Pellicer, J. Reklaitis, D. Baltrunas, H. Cesiulis, and J. Sort, *Mater. Des.* **139**, 429 (2018).
- ²⁴H. X. Yang, M. Chshiev, B. Dieny, J. H. Lee, A. Manchon, and K. H. Shin, *Phys. Rev. B* **84**, 054401 (2011).
- ²⁵T. Devolder, J. Ferré, C. Chappert, H. Bernas, J. P. Jamet, and V. Mathet, *Phys. Rev. B* **64**, 064415 (2001).
- ²⁶V. Jeudy, A. Mougin, S. Bustingorry, W. Savero Torres, J. Gorchon, A. B. Kolton, A. Lemaitre, and J. P. Jamet, *Phys. Rev. Lett.* **117**, 057201 (2016).
- ²⁷R. Diaz Pardo, W. Savero Torres, A. B. Kolton, S. Bustingorry, and V. Jeudy, *Phys. Rev. B* **95**, 184434 (2017).
- ²⁸J. Ferré, V. Repain, J. P. Jamet, A. Mougin, V. Mathet, C. Chappert, and H. Bernas, *Phys. Status Solidi A* **201**, 1386 (2004).
- ²⁹S. G. Je, D. H. Kim, S. C. Yoo, B. C. Min, K. J. Lee, and S. B. Choe, *Phys. Rev. B* **88**, 214401 (2013).
- ³⁰M. Yamanouchi, A. Jander, P. Dhagat, S. Ikeda, F. Matsukura, and H. Ohno, *IEEE Magn. Lett.* **2**, 3000304 (2011).
- ³¹S. Jaiswal, K. Litzius, I. Lemesch, F. Büttner, S. Finizio, J. Raabe, M. Weigand, K. Lee, J. Langer, B. Ocker, G. Jakob, G. S. D. Beach, and M. Kläui, *Appl. Phys. Lett.* **111**, 022409 (2017).
- ³²R. Soucaille, M. Belmeguenai, J. Torrejon, J.-V. Kim, T. Devolder, Y. Roussigné, S.-M. Chérif, A. A. Stashkevich, M. Hayashi, and J.-P. Adam, *Phys. Rev. B* **94**, 104431 (2016).
- ³³H. Yang, O. Boule, V. Cros, A. Fert, and M. Chshiev, *Sci. Rep.* **8**, 1 (2018).
- ³⁴S. Tacchi, R. E. Troncoso, M. Ahlberg, G. Gubbiotti, M. Madami, J. Åkerman, and P. Landeros, *Phys. Rev. Lett.* **118**, 147201 (2017).
- ³⁵S. Peng, D. Zhu, J. Zhou, B. Zhang, A. Cao, M. Wang, W. Cai, K. Cao, and W. Zhao, *Adv. Electron. Mater.* **5**, 1900134 (2019).
- ³⁶A. Belabbes, G. Bihlmayer, F. Bechstedt, S. Blügel, and A. Manchon, *Phys. Rev. Lett.* **117**, 247202 (2016).
- ³⁷G. W. Kim, A. S. Samardak, Y. J. Kim, I. H. Cha, A. V. Ognev, A. V. Sadovnikov, S. A. Nikitov, and Y. K. Kim, *Phys. Rev. Appl.* **9**, 64005 (2018).